Journal of Visualized Experiments

Oxygen-Induced Retinopathy Model for Ischemic Retinal Diseases in Rodents

--Manuscript Draft--

Article Type:	Invited Methods Article - JoVE Produced Video
Manuscript Number:	JoVE61482R3
Full Title:	Oxygen-Induced Retinopathy Model for Ischemic Retinal Diseases in Rodents
Section/Category:	JoVE Medicine
Keywords:	Angiogenesis, neovascularization, oxygen-induced retinopathy, hypoxia, retinopathy of prematurity, diabetic retinopathy, intravitreal injection, image analysis, artificial intelligence
Corresponding Author:	Tero Järvinen Tampereen Yliopisto Tampere, Pirkanmaa FINLAND
Corresponding Author's Institution:	Tampereen Yliopisto
Corresponding Author E-Mail:	tero.jarvinen@tuni.fi
Order of Authors:	Tero Järvinen
	Maria Vähätupa
	Hannele Uusitalo-Järvinen
	Giedrius Kalesnykas
	Marc Cerrada-Gimenez
	Niina Jääskeläinen
	Rubina Thapa
Additional Information:	
Question	**Response**
Please indicate whether this article will be Standard Access or Open Access.	Standard Access (US$2,400)
Please indicate the **city, state/province, and country** where this article will be **filmed**. Please do not use abbreviations.	Tampere, Finland

TITLE:

Oxygen-Induced Retinopathy Model for Ischemic Retinal Diseases in Rodents

AUTHORS AND AFFILIATIONS:

Maria Vähätupa[1,2], Niina Jääskeläinen[2], Marc Cerrada-Gimenez[2], Rubina Thapa[2], Tero A.H. Järvinen[1], Giedrius Kalesnykas[2], Hannele Uusitalo-Järvinen[1,3]

[1]Faculty of Medicine and Health Technology, Tampere University & Tampere University Hospital, Tampere, Finland
[2]Experimentica Ltd, Kuopio, Finland
[3]Eye Centre, Tampere University Hospital, Tampere, Finland

Corresponding author:
Hannele Uusitalo-Järvinen (hanne.uusitalo-jarvinen@tuni.fi)

Email addresses of co-authors:
Maria Vähätupa (maria.vahatupa@tuni.fi)
Niina Jääskeläinen (niina.jaaskelainen@experimentica.com)
Marc Cerrada-Gimenez (marc@experimentica.com)
Rubina Thapa (rubina.thapa@experimentica.com)
Tero A.H. Järvinen (tero.jarvinen@tuni.fi)
Giedrius Kalesnykas (giedrius.kalesnykas@experimentica.com)

KEYWORDS:
angiogenesis, neovascularization, oxygen-induced retinopathy, OIR, hypoxia, retinopathy of prematurity, ROP, diabetic retinopathy, intravitreal injection, image analysis, artificial intelligence, AI

SUMMARY:
Oxygen-induced retinopathy (OIR) can be used to model ischemic retinal diseases such as retinopathy of prematurity and proliferative diabetic retinopathy and to serve as a model for proof-of-concept studies in evaluating antiangiogenic drugs for neovascular diseases. OIR induces robust and reproducible neovascularization in the retina that can be quantified.

ABSTRACT:
One of the commonly used models for ischemic retinopathies is the oxygen-induced retinopathy (OIR) model. Here we describe detailed protocols for the OIR model induction and its readouts in both mice and rats. Retinal neovascularization is induced in OIR by exposing rodent pups either to hyperoxia (mice) or alternating levels of hyperoxia and hypoxia (rats). The primary readouts of these models are the size of neovascular (NV) and avascular (AVA) areas in the retina. This preclinical in vivo model can be used to evaluate the efficacy of potential anti-angiogenic drugs or to address the role of specific genes in the retinal angiogenesis by using genetically manipulated animals. The model has some strain and vendor specific variation in the OIR

induction which should be taken into consideration when designing the experiments.

INTRODUCTION:

Reliable and reproducible experimental models are needed to study the pathology behind angiogenic eye diseases and to develop novel therapeutics to these devastating diseases. Pathological angiogenesis is the hallmark for wet age-related macular degeneration (AMD) and for many ischemic retinal diseases among them retinopathy of prematurity (ROP), proliferative diabetic retinopathy (PDR) and retinal vein occlusion (RVO)[1-4]. Human and rodent retinas follow a similar pattern of development, as both human and rodent retina are among the last tissues that are vascularized. Before the retinal vasculature has completely developed, retina receives its nutrient supply from hyaloid vasculature, which, in turn, regresses when the retinal vasculature starts to develop[1,2]. In human, retinal vascular development is completed before birth, whereas in rodents the growth of retinal vasculature occurs after birth. Since the retinal vascular development occurs postnatally in rodents, it provides an ideal model system to study the angiogenesis procedure[2,3]. The newborn rodents have an avascular retina that develops gradually until complete vascular retina development is achieved by the end of third postnatal week[4]. The growing blood vessels of neonatal mouse are plastic, and they undergo regression during hyperoxia stimulus[5].

ROP is the leading cause for childhood blindness in Western countries, as it affects almost 70% of the premature infants with birthweight under 1,250 g[6,7]. ROP occurs in premature infants who are born before retinal vessels completes their normal growth. ROP progresses in two phases: in Phase I, preterm birth delays the retinal vascular growth where after in phase II, the unfinished vascularization of the developing retina causes hypoxia, which induces the expression of angiogenic growth factors that stimulate new and abnormal blood vessel growth[8]. The OIR model has been a widely used model to study the pathophysiology of ROP and other ischemic retinopathies as well as to test novel drug candidates[2,3,9]. It is widely considered as a reproducible model for carrying out proof-of-concept studies for potential antiangiogenic drugs for ocular as well as non-ocular diseases. The two rodent models i.e., mouse and rat OIR differ in their model induction and disease phenotype. The rat model mimics ROP phenotype more accurately, but the mouse model provides more robust, fast and reproducible model for retinal neovascularization (NV). In the mouse model, NV develops to the central retina. This pathological read-out is important in pharmacologic efficacy studies for many ischemic retinopathies, such as PDR, RV and exudative AMD as well as for non-ocular, angiogenic diseases such as cancer. Moreover, availability of genetically manipulated (transgenic and knockout) mice makes the mouse OIR model a more popular option. However, neither mouse nor rat OIR model creates retinal fibrosis, which is typical in human diseases.

The understanding that high oxygen levels contribute to the development of ROP in 1950s[10,11] led to the development of animal models. The first studies about the effect of oxygen for retinal vasculature were done in 1950[12-14] and until the 1990s there were many refinements to the OIR model. The research by Smith et al. in 1994 set a standard for a current mouse OIR model that separates hyaloidopathy from retinopathy[15]. A wide adoption of the method to quantify vaso-obliteration and pathological NV by Connor et al. (2009) further increased its popularity[16]. In this

model, mice are placed at 75% oxygen (O_2) for 5 days at P7, followed by 5 days in normoxic conditions. Hyperoxia from P7 to P12 causes retinal vasculature to regress in central retina. Upon return to room air, avascular retina becomes hypoxic (**Figure 1A**). Due to the hypoxic stimuli of the avascular central retina, some of the retinal blood vessels sprout towards the vitreous, forming preretinal NV, called preretinal tufts[2,3]. These tufts are immature, and hyperpermeable. The amount of NV peaks at P17, after which it regresses. The retina is fully revascularized and NV is fully regressed by P23 - P25 (**Figure 2A**)[2,3].

The rat OIR model (using varying levels of O_2) was first described in the 1990s showing that varying O_2 levels at 80% and 40% cause more pronounced NV than under 80% O_2 constant exposure[17]. Later it was discovered that the intermittent hypoxia model, where O_2 is cycled from hyperoxia (50%) to hypoxia (10-12 %), causes even more NV than the 80/40% O_2 model[18]. In the 50/10% model, rat pups are exposed to 50% for 24 hours, followed by 24 hours in 10% O_2. These cycles are continued until P14, when the rat pups are returned to normoxic conditions **(Figure 1B**). As in human ROP patients, in the rat model the avascular areas develop to the periphery of retina because of immature retinal vascular plexus (**Figure 3**).

In both models, the main parameters that are usually quantified are the size of AVA and NV. These parameters are typically analyzed from retinal flat mounts where the endothelial cells are labeled[4,16]. Previously the amount of preretinal NV was evaluated from retinal cross sections by counting blood vessel or vascular cell nuclei extending to vitreous above the inner limiting membrane. The major limitation of this approach is that it is not possible to quantify the AVAs.

PROTOCOL:

The protocol described here has been approved by the National Animal Ethics Committee of Finland (protocol number ESAVI/9520/2020 and ESAVI/6421/04.10.07/2017).

1. Experimental animals and mouse OIR model induction

NOTE: Use time-mated animals, e.g., commonly used C57BL/6J mice, to get pups born on the same day. Use fostering dams, e.g., 129 strain (129S1/SvImJ or 129S3/SvIM) lactating dams, to nurse the pups during and after the induction of hyperoxia. Alternatively, make sure that there are extra lactating dams available in case the nursing dams need to be replaced due to exhaustion. Restrict the litter size to 6-7 pups for each dam when using C57BL/6J mice/dams (if the litters are larger than that the pups tend to have restricted weigh gain)[16].

1.1. Record the weight of the animals before and after hyperoxia induction, and at the time of sacrifice.

1.2. Make sure that there is enough food on the bottom of the cage, so the dams have an easy access to food.

1.3. Add soda lime with color indicator to the bottom of the chamber to absorb excess CO_2 when a filtration system is not used.

1.4. Monitor the humidity and temperature inside the chamber and keep the humidity between 40 to 65%. Increase the humidity of the chamber, if needed, by placing dishes with water on bottom of the chamber (e.g., Petri dishes).

1.5. Calibrate the O_2 sensor with 100% O_2 and normal room air.

1.6. Place the P7 mice into a chamber and set up the O_2 level to 75%. Keep the mice in the chamber for 5 days, until P12. Avoid opening the chamber during the hyperoxia induction. Check the gas pressure of the O_2 cylinder and replace the cylinder when needed. Monitor the animals during the induction.

1.7. Take the mouse cages out of the chamber and weigh all the pups. Group the pups based on the weight so that each experimental group has similar weigh distribution in pups.

2. Experimental animals and rat OIR model induction (using semi-closed system)

NOTE: Use time-mated animals to get the pups born on the same day. For rat OIR, use increased litter size, approximately 18 pups/dam, to obtain sufficient NV induction in the rat model. Pool pups from several litters to obtain enough pups to each litter.

2.1. Record the weight of the animals before and after induction, and at the time of sacrifice.

2.2. Make sure that there is enough food on the bottom of the cage, so the dams have an easy access to food.

2.3. Add soda lime with color indicator to the bottom of the chamber to absorb excess CO_2 when filtration system is not used.

2.4. Monitor the humidity and temperature inside the chamber. Absorb extra humidity (generated from multiple number of rats) by adding silica gel on the bottom of chamber.

2.5. Calibrate the O_2 sensor with 100% N_2 and normal room air.

2.6. Place the rats into the chamber at P0 (few hours after the birth). Set the O_2 level to 50% and connect O_2 cylinder to the chamber for 24 h. After that, switch the settings to 10% O_2 and connect nitrogen (N_2) cylinder to the chamber for 24 h. Continue the 24 h cycling between 50% and 10% O_2 levels for 14 days.

2.7. Monitor the gas consumption and the wellbeing of the animals during the study. Open the chamber during the change between 50/10% O_2 and add more food and water if needed. Change the cages of the animals to clean ones during the induction.

2.8. Take the rat cages out of the chamber and weigh all the pups. Group the pups based on

the weight so that each experimental group has similar weigh distribution in the pups.

3. Drug administration (optional)

NOTE: Commonly used drug administration route in OIR is by intravitreal treatment (ivt), at P12-P14 for mice and at P14 for rats. Determine the treatment day based on the experimental setup. When multiple litters of pups are used in experiments, divide the treatment groups to have animals from all the litters. Preferably, inject the drug to only one eye, and keep the contralateral eye as a control.

3.1. Weigh the animals and make identifications marks to the tail and/or ear.

3.2. Anesthetize the animal either with injectable anesthesia (for example mixture of ketamine and medetomidine, 30 mg/kg and 0.4 mg/kg for mice) or with inhalation anesthesia (isoflurane at 2-3.5% isoflurane and 200-350 mL/min air flow). Check the depth of the anesthesia by pinching the toes. Keep the animal on a heating pad during the treatment.

3.3. For local anesthesia, apply a drop of analgesic onto the eyelid. Open the eyelid carefully with forceps before performing the ivt, as mice and rats open their eyes around P14. Apply a drop of analgesic (e.g., oxybuprocaine hydrochloride) onto the cornea.

3.4. Apply a drop of iodine before conducting the ivt injection.

3.5. For the ivt injection use a glass syringe with a 33-34 G needle attached. Press the eyelids down and grap the eyeball with forceps. Make the injection posterior to the limbus, approximately in 45˚ angle needle pointing towards optic nerve.

3.6. Avoid injecting more than 1.0 µL of PBS (+ drugs) into the intravitreal space. Keep the needle in place for 30 s after injecting the drug to avoid reflux of the injected solution.

3.7. Examine the eye (e.g., with an ophthalmoscope) for any complications, such as hemorrhages or retinal damage, after removing the needle. Apply antibiotic ointment on top of cornea after the injection.

NOTE: The ivt injection volume for mice should be 0.5 – 1.0 µL (PBS, not saline).

3.8 Reverse the anesthesia (for example with an α2-antagonist for medetomidine (2.5 mg/kg) and return the pup to the cage. House the litter normally until the end of the study.

4. In vivo imaging and electroretinography (optional)

4.1. If desired, conduct in vivo imaging on live animals during the follow-up period to record changes that develop in retina during the angiogenic responses. For example, perform fluorescein angiography (FA) or scanning laser confocal microscopy[19] to visualize the vasculature

(**Figure 4**). Use spectral domain optical coherence tomography (SD-OCT) to visualize retinal layers in vivo (**Figure 4**).

4.2. If desired, investigate functional changes in different retinal cell populations after OIR induction by using electroretinography (ERG) **(Figure 5**).

5. Tissue collection and preparation of retinal flat mounts

NOTE: Collect the tissues according to the desired research hypothesis. For mice, collect the samples for example at P12 (to study vaso-obliteration after the hyperoxic phase) or at the hypoxic period (P13-P17). Collect the mouse OIR samples at P17, which is the most common time point for sampling, to detect the peak in NV amount. In rat OIR, collect the samples at P18-P21 to observe the highest amount of NV (**Figure 3**).

5.1. Weigh the animals before sampling.

5.2. To label the retinal vasculature, deeply anesthetized animals can be transcardially perfused with FITC-dextran. (Alternatively, stain the retinal flat mounts with Isolectin later).

5.3. Sacrifice the animals using either overdose of anesthesia drugs (for example mixture of ketamine and medetomidine, 300 mg/kg and 4 mg/kg for mice) or CO_2 inhalation.

5.4. Collect the eyes of the animals by grabbing behind the eyeball with curved forceps, cut the tissue around the eyes and lift the eye out from the orbit.

5.5. Incubate the eyeballs in freshly made, filtered 4% paraformaldehyde (in phosphate-buffered saline, PBS) for 1-4 h. Remove the fixative and wash the eyeballs 3 x 10 min with PBS. Dissect the retinas immediately or store them in PBS at +4 °C.

CAUTION: Paraformaldehyde is toxic by inhalation, in contact with skin and if swallowed. Please read safety data sheet before working with it.

NOTE: Do not apply pressure to the eyeball during the sampling or any phase of the tissue processing in order to avoid retinal detachment, if cross-sections from whole eyeballs are done.

5.6. Prepare retinal flat mounts to quantify the amount of NV and the size of AVAs. Alternatively, process the eyeballs/retinas for histology, or RNA or protein analysis. Dissect the retina under a stereo microscope using micro scissors and forceps.

5.6.1. Place the eyeball in PBS to keep it moist and puncture the eyeball at limbus with needle (23G) and cut around limbus with curved micro scissors to remove iris and the cornea.

5.6.2. Carefully place the tip of the scissors between sclera and retina and cut sclera towards the optic nerve. Do the same to the other side of the eyeball, and carefully cut/tear the sclera

until the retinal cup is exposed. Pull the lens out from the retinal cup and add PBS to the cup.

5.6.3. Remove all the hyaloid vessels, vitreous and debris without damaging the retina. Wash the retina by adding PBS to the retinal cup. Perform four incision (at 12, 3, 6 and 9 o'clock) to the retina with straight micro scissors to make a flower-like structure. Optionally, make the cuts with surgical blade prior mounting the samples. Lift the retina using a soft paintbrush to a well-plate for staining.

5.7. Label the retinal vasculature using Isolectin B_4 which stains the surface of endothelial cells (if the animals were not perfused with FITC-dextran). Incubate the retinas in blocking buffer (10% NGS + 0.5% Triton in TBS) for 1 h and wash with 1% NGS + 0.1% Triton in TBS for 10 min. Incubate the retinas with fluorescent dye conjugated Isolectin B_4 (5-10µg/ml) in 1% NGS + 0.1% Triton in TBS overnight at +4 ° C while protected from the light.

NOTE: If desired, label other cells such as inflammatory cells and pericytes using specific antibodies.

5.8. Wash the retinas 3x for 10 min with 1% NGS + 0.1% Triton in TBS and lift retinas on a microscopic slide, inner retina facing upwards. Carefully spread out the retina using soft paintbrush and remove any remaining hyaloid vessels or debris. Add mounting medium to a cover slip and place it on top of the retina. Store retinas at 4 °C and protect from light.

6. Analysis of the flat mounts

6.1. Imagine the retinal flat mounts using fluorescence microscope with 10x objective. Focus to the superficial vascular plexus and to the preretinal neovascularization. Make a tile scan image to capture the whole retina and merge the tile scans

6.2. Quantify the images by measuring the AVAs, area of neovascularization and total retinal area using an image processing program (see **Table of Materials**).

6.2.1. Draw the AVAs and total retinal area using a free hand drawing tool and select the neovascular areas using a selection tool. The software measures the regions of interest in pixels, and the AVA and NV areas (expressed in pixels) can be used to calculate their percentage in relation to the total retinal area. Also, some software tools are available for quantifying NV.

NOTE: Recently, an open-source, fully automated pipelines for the quantification of key values of OIR images using deep learning neural networks have been introduced and provide a reliable tool for reproducible quantification of retinal AVA and NV (e.g., https://github.com/uw-biomedical-ml/oir/tree/bf75f9346064f1425b8b9408ab792b1531a86c64)[20,21].

6.3. If using antibodies for immunohistochemical detection of individual cell populations, quantify the number of stained cells (such as microglia, **Figure 2B**) from the retinal flat mounts by hand or by automated image analysis systems if desired.

7. Statistics

7.1. Analyze normally distributed data by Student's t test or One-Way ANOVA followed by Dunnett's or Tukey's multiple comparisons test, as appropriate. Use nonparametric tests like Mann-Whitney U test or Kruskal Wallis test for non-normally distributed data. Consider differences statistically significant at the $P < 0.05$ level.

REPRESENTATIVE RESULTS:

The main outcome of the model is the vascular phenotype: the size of AVAs and the amount of NV. In the mouse OIR model, the vaso-obliteration occurs in the central retina (**Figure 2A**), while in the rat model it develops in the periphery, i.e., similar to human ROP[22] (**Figure 3A**). This is because the superficial vascular plexus has already developed when mice are exposed to hyperoxia, whereas in the rat model the retina is avascular at the time of OIR induction (P0). Preretinal neovascularization develops near the avascular areas, i.e., central retina in mouse, and periphery in rats (**Figure 2A** and **Figure 3A**).

Histological analysis using either cross-sections or flat mounts can be done to evaluate morphological changes in OIR retinas or the presence of cell types of interest, for example inflammatory cells (**Figure 2B**). In addition to retina, whole eye or vitreous samples can be collected for further gene and protein expression analyses in different time points during the OIR model. Gene or protein expression levels can be analyzed with standard methods, such as RT-qPCR or western Blotting.

Optionally, non-invasive in vivo imaging can be conducted during the OIR follow-up period. Retinal and hyaloid vasculature can be visualized with FA (**Figure 4A**). SD-OCT can be used to evaluate structural changes in the retina (**Figure 4B**). Functional changes in retina can be measured by ERG (**Figure 5**).

Inhibitors of vascular endothelial growth factor (VEGF) are commonly used in the treatment of human angiogenic eye diseases. Thus, anti-VEGF is often used as a reference compound in OIR. Aflibercept, that works as a soluble VEGF-trap, inhibits both NV and physiological revascularization in OIR in both high and low doses (injected at P14). OIR eyes injected at P14 with high dose of aflibercept had even bigger retinal AVAs than untreated eyes (**Figure 6**). This suggests that aflibercept blocks also physiological retinal revascularization driven by hypoxia. Both mouse and rat models can be used to evaluate the effect of different anti-angiogenic agents on retinal NV and physiological revascularization of the retina (**Figure 3B** and **Figure 6**).

FIGURE LEGENDS:

Figure 1: Graphical overview of a standard OIR study design for mice and rats. (**A**) Mouse OIR model was induced by exposing the mice to 75% O_2 from P7 to P12 and returned to normal room air. The peak of preretinal NV was seen at P17, which was usually the sampling point for the experiment. (**B**) Rat OIR model was induced by exposing the rats to alternating O_2 levels (50/10 % O_2) from P0 to P14 and returned to normoxic conditions. Rats were usually sacrificed at P20,

when the amount of NV peaked.

Figure 2: Vascular phenotype in the mouse OIR model. Mouse OIR model was generated as described in Figure 1. (**A**) The superficial vascular plexus developed in normal mice while the OIR mice were exposed for 75% O_2 from P7 to P12. During this time, vascular obliteration developed in the central retina (marked in blue at P12 and P17 in the lower panel). Mice were returned to normal room air, and the avascular retina became hypoxic, leading to functional vessel regrowth in retina and pathological NV (marked in red at P17 in the lower panel). The amount of NV peaked at P17 and regressed afterwards. Retina was fully revascularized and the NV regressed around P24-P25. Preretinal neovascular tufts developed between the vascular and avascular areas in central retina. (**B**) An example of immunohistochemical staining of retinal flat mount showing retinal Iba-1 stained microglia (green) and GS-IB_4 stained blood vessels (red) at P12 and P17. (**C**) Cross-section of mouse OIR retina at P17, where preretinal tufts (arrows) were sprouting towards the vitreous. Also, thinning of the inner nuclear layer (INL) and outer plexiform layer (OPL) wre seen. Scale bars are 1 mm in A, 50 µm in B, and 100 µm in C. ILM = inner limiting membrane, GCL = ganglion cell layer, IPL = inner plexiform layer, INL = inner nuclear layer, OPL = outer plexiform layer, ONL = outer nuclear layer, RPE = retinal pigment epithelium.

Figure 3: Vascular phenotype and its development in the rat OIR model. (**A**) Avascular areas (marked in blue) and NV (marked in red) developed in the periphery of the retina, similar to human ROP. (**B**) AVAs were seen in OIR retinas, but not in normoxic controls. (**C**) Quantification of the area of NV showed a trend towards a peak in the amount of the NV at P20, but the difference was not statistically significant compared to P18 and P21 in OIR. (Student's t-test, ** $p \leq 0.01$, *** $p \leq 0.001$, both eyes of the animals plotted in the graph).

Figure 4: In vivo imaging using fluorescein angiography (FA) and spectral domain optical coherence tomography (SD-OCT) in the rat OIR model. (**A**) Vascular tortuosity (arrowheads) was seen in the images taken from the central retina (top row) at P18 and P20 in OIR rats compared to normoxic P19 rats. NV (arrows) and AVAs (asterisk) developed to the periphery of the retina (middle row) as seen in P18 and P20 OIR retinas. Regressing hyaloid vessels (bottom row) were captured by FA. (**B**) Blood vessel growth towards the vitreous was observed as a thickening on the nerve fiber layer (NFL) and ganglion cell layer (GCL) in the OIR retinas (arrow).

Figure 5: Functionality of retinal neurons can be measured using flash electroretinography (fERG). (**A**) a-waves were derived from retinal cone and rod photoreceptors and their amplitudes were significantly decreased in the rat OIR model. The effect increased with a higher light intensity, suggesting that the defects were affecting cone photoreceptor functions primarily. (**B**) B-wave amplitudes from OIR animals were decreased compared to normoxic controls. B-waves were derived from ON-bipolar cells and Müller cells.

Figure 6: Intravitreally injected PBS reduces NV and AVAs in the mouse OIR model. (**A**) Representative images of retinal flat mounts from untreated, and aflibercept-treated (20 µg at P14) and PBS injected OIR eyes at P17. High dose of aflibercept (20 µg) increased the size of AVAs by 47% (outlined in white) and inhibited NV by 98% (arrows) compared to untreated controls.

PBS injected decreased AVAs by 31% and NV by 42% compared to untreated controls. Also, puncture of the sclera resembling ivt produced similar effects as ivt injection of PBS, but the differences were not statistically significant. Arrowhead points at hyaloid vessels that were not removed during the dissection. (One-Way ANOVA, * $p \leq 0.05$; ** $p \leq 0.01$, *** $p \leq 0.001$, **** $p \leq 0.0001$).

DISCUSSION:

The severity of disease phenotype is dependent on both the strain and even vendor in both mouse and rat OIR models[23]. This suggests that there is a wide genotypic variability in the pathology development. In general, pigmented rodents develop more severe phenotype than the albino ones. For example, the retinal vasculature of albino BALB/c revascularizes rapidly after hyperoxia and does not develop NV at all[24]. Similarly, in rats, pigmented Brown Norway rats show more severe pathology than albino Sprague Dawley (SD) rats[25]. SD rats are commonly used strain, and vendor-related differences in OIR phenotype have been reported within the strain. For example, SD rats f produce significantly more NV than rats[23]. C3H/HeJ mice, in turn, that have a mutation in the retinal degeneration 1 (*Rd1*) gene. They have thin retinas and do not develop NV[26]. Due to these reasons and the availability of transgenic mice lines, the inbred C57BL/6J is the most commonly used mouse strain for OIR studies. However, there is quite a high mortality among the C57BL/6J dams due to the hyperoxic exposure, so the wellbeing of the mice needs to be considered when designing the study and monitored during the experiments. Moreover, increased photoreceptor damage is seen in C57BL/6 mice compared to BALB/c mice [27].

In order to ensure the wellbeing of the mice and survival of the dams and pups, the litter size should be kept small (6-7 pups/dam). This is especially important when using C57BL/6 mice, which are more susceptible to hyperoxic stress[27,28]. In addition, easily accessible support food (placed on the bottom of the cage) should be provided to the mice. Some researchers use surrogate dams to replace the dams in the chamber with healthy ones after the oxygen-induction. However, most researchers use surrogates only if the dam is exhausted[22,29]. Surrogate dams are recommended to be used if bigger litter sizes are used. It has been published that 129S3/SvIM mice produce more NV than C57BL/6 and sustain better the changes caused by varying oxygen levels[28]. It should be noted that the dams used in OIR are unfertile after the OIR induction and should not be used for further breeding purposes[22]. Postnatal weight gain of the pups affects the severity of OIR pathology. Pups with poor postnatal weight gain (<5 g at P17) show delayed expression of VEGF and thus prolonged phase of retinopathy when compared to pups with normal (5 - 7.5 g at P17) or extensive weight gain (>7.5 g at P17) [29]. Furthermore, mice pups weighing over 5 g at P7 do not show vaso-obliterated areas after OIR induction[30]. Thus, it is important to weigh the pups during the experiment. The contralateral untreated eye can be used as an internal control to ensure that the nutritional status of the mice does not affect the results. The situation is similar in rats; the smaller the pups are, the more severe OIR phenotype they develop[31]. Thus, large litter size (approx. 18 pups) are recommended to be used for the rat OIR model.

The OIR model induction can be done using either fully closed system, where there is a closed-loop circuit with a pump that circulates the air through a filter system (soda lime and activated

carbon) back to the chamber. Another option is a semi-closed system, where ventilation ensures that the excess metabolites are removed from the chamber. To ensure that excess CO_2 is removed, soda lime (mixture of calcium hydroxide with sodium hydroxide or potassium hydroxide) can be placed on the bottom of the chamber. The removal of CO_2 is mandatory as the high CO_2 levels worsen the disease phenotype in rats[32]. One should also remember to recalibrate the oxygen sensor of the chamber regularly as they tend to drift over time and may provide wrong oxygen concentration from one intended.

It has been reported that vehicle injection (PBS) alone or even just the puncture to the intravitreal space has an effect for the revascularization rate and the amount of NV (**Figure 6**)[33-36]. It has been speculated whether the effect seen with PBS/vehicle injection could be due to changes in intraocular pressure during injection, or due to injury to ocular structures that increases levels of angiogenic growth factors among them pigment epithelium-derived growth factor[34,37]. Furthermore, just a pilot subretinal injection alone (puncture to the subretinal space) has been shown to have effects on the vascular and functional phenotype in OIR when compared to the untreated rats[38]. These results highlight the importance of proper negative controls in the OIR studies or even systemic administration of tested compounds, as well as big enough n-numbers in each study group. The fact that vehicle injection indeed enhances revascularization rate in retina is a major limiting factor as the revascularization rate and the formation of pathological preretinal tufts are inter-related in the OIR model: if the revascularization rate is accelerated, it leads to the compensatory downregulation of neovascular tufts and vice versa. Thus, both primary outcome measures of OIR model are affected by vehicle injection.

VEGF inhibitors have revolutionized the treatment AMD and DR. OIR model was used to demonstrate their efficacy preclinically. Concerning VEGF inhibitors in OIR, a study comparing different anti-VEGFs and anti-PlGFs (placental growth factor) (injected at P12) showed that anti-VEGF alone led to small avascular areas, whereas anti-PlGF treated eyes had bigger avascular areas[33]. Aflibercept had the biggest AVAs when compared to other drug treatments[33]. Aflibercept is known to bind both VEGF and PlGF[39], it could be that inhibiting PlGF in OIR leads to blocking of physiological angiogenesis.

Noninvasive in vivo imaging provides a tool for monitoring retinal vasculature[40] and retinal layers and structure during follow-up period. Using FA, parameters like vascular density and vascular tortuosity (plus disease, **Figure 4A**) can be measured[40,41]. SD-OCT can be used for evaluating structural changes and measuring retinal thickness during OIR follow-up period[42,43]. ERG is used to measure the functional changes in the retina. Different cell types produce signals after light stimulus, and these signals or “waves” can be measured with ERG. Photoreceptors are producing the negative a-wave, and ON bipolar cells and Müller cells are mainly responsible for the b-wave[44]. Loss of retinal function is typical in OIR mice and rats[45,46] (**Figure 5**). Long lasting changes persist in retina and both functional changes and changes in protein level have been reported in OIR retinas even after revascularization and NV regression[34,47].

To visualize the retinal vasculature, the live mice can be either perfused with FITC-labeled dextran or the retinal flat mounts can be stained with fluorescent dye labeled Isolectin B_4. One needs to

understand the difference between the fluorescent dyes; the perfusion with FITC-dextrans labels only the lumen of the vessels, whereas Isolectin B_4 stains the surface of endothelial cells. Thus, functional blood vessels with proper lumen will only be visualized with FITC-dextran perfusion, while the total area of NV appears bigger in Isolectin B_4 stained retinas than in FITC-dextran perfused animals, because Isolectin B_4 essentially picks up even endothelial cells which have not formed functional lumens yet[48]. One future option to visualize whole retina/eye ball in 3-D format is deep tissue imaging by two-photon fluorescence microscopy [(49)].

The rodent OIR model, as well as the animal models in general, only partially represent the characteristics of human diseases. The major difference related to OIR is that retinal neovascularization is not associated with fibrosis in rodent OIR, whereas retinal neovascularization leads commonly to fibrovascular proliferation in human neovascular retinal diseases. Furthermore, the conditions that cause OIR vs. human disease can be almost opposite. The preterm neonates with ROP require supplemental oxygen with respiratory support, experience frequently intermittent hypoxemic and hyperoxemic episodes caused by recurrent apnea, but they are not exposed to high level of oxygen. To minimize the permanent damage, high fractions of inspired O_2 are avoided. In that respect, neither the mouse model with constant exposure to 75% O_2 for 5 days nor the 50/10 rat model resemble pathogenesis of human ROP. Furthermore, there are also differences between the rat and the mouse OIR models. The neovascularization regresses in the mouse model with re-establishment of normal vessels by P24, whereas the condition gets worse in the rat OIR model (similar to human ROP). Although, the rat OIR model shows clinically relevant features of ROP such as the delayed retinal vascular development and subsequent pathological neovascularization, its use is limited by almost complete absence of transgenic rat strains, higher maintenance expenses and less NV than in the mouse OIR model.

Taken together, despite the differences between human ischemic proliferative retinopathies and rodent OIR models, the ease by which the NV can be induced, coupled with easy visualization and quantification of the retina, make the OIR models popular to study the molecular mechanisms and potential therapeutics for ischemic proliferative retinopathies. Interestingly, the hyperoxia exposure in mouse OIR model also induces bronchopulmonary dysplasia, another disease caused by supplemental oxygen therapy in human premature infants, showing that OIR model could be used to explore novel targets for both ROP and bronchopulmonary dysplasia simultaneously[50].

ACKNOWLEDGMENTS:

We thank Marianne Karlsberg, Anne Mari Haapaniemi, Päivi Partanen and Anne Kankkunen for excellent technical support. This work was funded by the Academy of Finland, Päivikki and Sakari Sohlberg Foundation, Tampere Tuberculosis Foundation, Finnish Medical Foundation, Pirkanmaa Hospital District Research Foundation and the Tampere University Hospital Research Fund.

DISCLOSURES:

The authors Maria Vähätupa, PhD, Niina Jääskeläinen, Marc Cerrada-Gimenez, PhD, and Rubina Thapa are employees of Experimentica Ltd.

The author Giedrius Kalesnykas, PhD, is an employee (President and Chief Executive Officer) and shareholder of Experimentica Ltd. that offers contract research services employing preclinical OIR models used in this Article.

Tero Järvinen, M.D., PhD, and Hannele Uusitalo-Järvinen, M.D., PhD, have nothing to disclose.

REFERENCES:

1. Chase, J. The evolution of retinal vascularization in mammals. A comparison of vascular and avascular retinae. *Ophthalmology*. **89** (12), 1518-1525 (1982).
2. Sun, Y., Smith, L. E.H. Retinal vasculature in development and diseases. *Annual Review of Vision Science*. **4**, 101-122 (2018).
3. Vähätupa, M., Järvinen, T. A. H., Uusitalo-Järvinen, H. Exploration of oxygen-induced retinopathy model to discover new therapeutic drug targets in retinopathies. *Frontiers in Pharmacology*. **11**, 873 (2020).
4. Stahl, A. et al. The mouse retina as an angiogenesis model. *Investigative Ophthalmology & Visual Science*. **51** (6), 2813-2826 (2010).
5. Benjamin, L. E., Hemo, I., Keshet, E. A plasticity window for blood vessel remodelling is defined by pericyte coverage of the preformed endothelial network and is regulated by PDGF-B and VEGF. *Development*. **125**(9), 1591-1598 (1998).
6. Bashinsky, A. L. Retinopathy of prematurity. *North Carolina Medical Journal*. **78** (2), 124-128 (2017).
7. Ludwig, C. A., Chen, T. A., Hernandez-Boussard, T., Moshfeghi, A. A., Moshfeghi, D. M. The epidemiology of retinopathy of prematurity in the united states. *Ophthalmic Surgery, Lasers and Imaging Retina*. **48** (7), 553-562 (2017).
8. Hartnett, M. E. Pathophysiology and mechanisms of severe retinopathy of prematurity. *Ophthalmology*. **122** (1), 200-210 (2015).
9. Liu, C. H., Wang, Z., Sun, Y., Chen, J. Animal models of ocular angiogenesis: From development to pathologies. *FASEB Journal*. **31** (11), 4665-4681 (2017).
10. Szewczyk, T. S. Retrolental fibroplasia; etiology and prophylaxis. *American Journal of Ophthalmology*. **35** (3), 301-311 (1952).
11. Szewczyk, T. S. Retrolental fibroplasia and related ocular diseases; classification, etiology, and prophylaxis. *American Journal of Ophthalmology*. **36** (10), 1336-1361 (1953).
12. Gerschman, R., Nadig, P. W., Snell, A. C. Jr., Nye, S. W. Effect of high oxygen concentrations on eyes of newborn mice. *American Journal of Physiology*. **179** (1), 115-118 (1954).
13. Gyllnesten, L. J., Hellström, B. E. Experimental approach to the pathogenesis of retrolental fibroplasia. III. changes in the eye induced by exposure of newborn mice to general hypoxia. *British Journal of Ophthalmology.* **39** (7), 409-415 (1955).
14. Curley, F. J., Habegger, H., Ingalls, T. H., Philbrook, F. R. Retinopathy of immaturity in the newborn mouse after exposure to oxygen imbalances. *American Journal of Ophthalmology*. **42** (3), 377-392 (1956).
15. Smith, L. E. et al. Oxygen-induced retinopathy in the mouse. *Investigative Ophthalmology & Visual Science*. **35** (1), 101-111 (1994).
16. Connor, K. M. et al. Quantification of oxygen-induced retinopathy in the mouse: A model

573 of vessel loss, vessel regrowth and pathological angiogenesis. *Nature Protocols*. **4** (11), 1565-1573
574 (2009).
575 17. Penn, J. S., Tolman, B. L., Lowery, L. A. Variable oxygen exposure causes preretinal
576 neovascularization in the newborn rat. *Investigative Ophthalmology & Visual Science*. **34** (3), 576-
577 585 (1993).
578 18. Penn, J. S., Henry, M. M., Tolman, B. L. Exposure to alternating hypoxia and hyperoxia
579 causes severe proliferative retinopathy in the newborn rat. *Pediatric Research*. **36** (6), 724-731
580 (1994).
581 19. Ritter, M. R. et al. Three-dimensional in vivo imaging of the mouse intraocular vasculature
582 during development and disease. *Investigative Ophthalmology & Visual Science*. **46** (9), 3021-
583 3026 (2005).
584 20. Xiao, S. et al. Fully automated, deep learning segmentation of oxygen-induced
585 retinopathy images. *Journal of Clinical Investigation Insight*. **2** (24) 97585 (2017).
586 21. Mazzaferri, J., Larrivee, B., Cakir, B., Sapieha, P., Costantino, S. A machine learning
587 approach for automated assessment of retinal vasculature in the oxygen induced retinopathy
588 model. *Scientific Reports*. **8** (1), 3916-018-22251-7 (2018).
589 22. Kim, C. B., D'Amore, P. A, Connor KM. Revisiting the mouse model of oxygen-induced
590 retinopathy. *Eye and Brain*. **8**, 67-79 (2016).
591 23. Barnett, J. M., Yanni, S. E., Penn, J. S. The development of the rat model of retinopathy of
592 prematurity. *Documenta Ophthalmologica*. **120** (1), 3-12 (2010).
593 24. Ritter, M. R. et al. Myeloid progenitors differentiate into microglia and promote vascular
594 repair in a model of ischemic retinopathy. *Journal of Clinical Investigation*. **116** (12), 3266-3276
595 (2006).
596 25. Floyd, B. N. et al. Differences between rat strains in models of retinopathy of prematurity.
597 *Molecular Vision*. **11**, 524-530 (2005).
598 26. Scott, A., Powner, M.B., Fruttiger, M. Quantification of vascular tortuosity as an early
599 outcome measure in oxygen induced retinopathy (OIR). *Experimental Eye Research*. **120**, 55-60
600 (2014).
601 27. Walsh, N., Bravo-Nuevo, A., Geller, S., Stone, J. Resistance of photoreceptors in the
602 C57BL/6-c2J, C57BL/6J, and BALB/cJ mouse strains to oxygen stress: Evidence of an oxygen
603 phenotype. *Current Eye Research*. **29** (6), 441-447 (2004).
604 28. Chan, C. K. et al. Differential expression of pro- and antiangiogenic factors in mouse strain-
605 dependent hypoxia-induced retinal neovascularization. *Laboratory Investigation*. **85** (6), 721-733
606 (2005).
607 29. Stahl, A. et al. Postnatal weight gain modifies severity and functional outcome of oxygen-
608 induced proliferative retinopathy. *American Journal of Pathology*. **177** (6), 2715-2723 (2010).
609 30. Liegl, R., Priglinger, C., Ohlmann, A. Induction and readout of oxygen-induced retinopathy.
610 *Methods in Molecular Biology*. **1834**, 179-191 (2019).
611 31. Holmes, J. M., Duffner, L. A. The effect of postnatal growth retardation on abnormal
612 neovascularization in the oxygen exposed neonatal rat. *Current Eye Research*. **15** (4), 403-409
613 (1996).
614 32. Holmes, J. M., Zhang, S., Leske, D. A, Lanier, W. L. The effect of carbon dioxide on oxygen-
615 induced retinopathy in the neonatal rat. *Current Eye Research*. **16** (7), 725-732 (1997).
616 33. Heiduschka, P., Plagemann, T., Li, L., Alex, A. F., Eter, N. Different effects of various anti-

617 angiogenic treatments in an experimental mouse model of retinopathy of prematurity. *Journal*
618 *of Clinical and Experimental Ophthalmology*. **47** (1), 79-87 (2019).
619 34. Tokunaga, C. C. et al. Effects of anti-VEGF treatment on the recovery of the developing
620 retina following oxygen-induced retinopathy. *Investigative Ophthalmology & Visual Science*. **55**
621 (3), 1884-1892 (2014).
622 35. Tokunaga, C. C, Chen, Y. H., Dailey, W., Cheng, M., Drenser, K. A. Retinal vascular rescue
623 of oxygen-induced retinopathy in mice by norrin. *Investigative Ophthalmology & Visual Science*.
624 **54** (1), 222-229 (2013).
625 36. Vähätupa, M., Uusitalo-Järvinen, H., Järvinen, T. A. H., Uusitalo, H., Kalesnykas, G.
626 Intravitreal injection of PBS reduces retinal neovascularization in the mouse oxygen-induced
627 retinopathy model. *Investigative Ophthalmology & Visual Science*. Abstract Issue, **57** (12) 3649
628 (2016).
629 37. Penn, J. S. et al. Angiostatic effect of penetrating ocular injury: Role of pigment
630 epithelium-derived factor. *Investigative Ophthalmology & Visual Science*. **47** (1), 405-414 (2006).
631 38. Becker, S., Wang, H., Stoddard, G. J., Hartnett, M. E. Effect of subretinal injection on
632 retinal structure and function in a rat oxygen-induced retinopathy model. *Molecular Vision*. **23**,
633 832-843 (2017).
634 39. Sophie, R. et al. Aflibercept: A potent vascular endothelial growth factor antagonist for
635 neovascular age-related macular degeneration and other retinal vascular diseases. *Biological*
636 *Therapy*. **2**, 3-012-0003-4 (2012).
637 40. Mezu-Ndubuisi, O. J. In vivo angiography quantifies oxygen-induced retinopathy vascular
638 recovery. *Optometry and Vision Science*. **93** (10), 1268-1279 (2016).
639 41. Mezu-Ndubuisi, O. J. et al. In vivo retinal vascular oxygen tension imaging and fluorescein
640 angiography in the mouse model of oxygen-induced retinopathy. *Investigative Ophthalmology &*
641 *Visual Science*. **54** (10), 6968-6972 (2013).
642 42. Dailey, W. A. et al. Ocular coherence tomography image data of the retinal laminar
643 structure in a mouse model of oxygen-induced retinopathy. *Data in Brief*. **15**, 491-495 (2017).
644 43. Mezu-Ndubuisi, O. J., Taylor, L. K., Schoephoerster, J. A. Simultaneous fluorescein
645 angiography and spectral domain optical coherence tomography correlate retinal thickness
646 changes to vascular abnormalities in an in vivo mouse model of retinopathy of prematurity.
647 *Journal of Ophthalmology*. **2017**, 9620876 (2017).
648 44. Pinto, L. H., Invergo, B., Shimomura, K., Takahashi, J. S., Troy, J. B. Interpretation of the
649 mouse electroretinogram. *Documenta Ophthalmologica*. **115** (3), 127-136 (2007).
650 45. Nakamura, S. et al. Morphological and functional changes in the retina after chronic
651 oxygen-induced retinopathy. *PLoS One*. **7** (2), e32167 (2012).
652 46. Dorfman, A. L., Polosa, A., Joly, S., Chemtob, S., Lachapelle, P. Functional and structural
653 changes resulting from strain differences in the rat model of oxygen-induced retinopathy.
654 *Investigative Ophthalmology & Visual Science*. **50** (5), 2436-2450 (2009).
655 47. Vähätupa, M. et al. SWATH-MS proteomic analysis of oxygen-induced retinopathy reveals
656 novel potential therapeutic targets. *Investigative Ophthalmology & Visual Science*. **59** (8), 3294-
657 3306 (2018).
658 48. Campos, M., Amaral, J., Becerra, S. P., Fariss, R. N. A novel imaging technique for
659 experimental choroidal neovascularization. *Investigative Ophthalmology & Visual Science*. **47**
660 (12), 5163-5170 (2006).

661 49. Yanez, C. O. et al. Deep Vascular Imaging in Wounds by Two-Photon Fluorescence
662 Microscopy. *PLos One.* **8** (7), e67559 (2013).
663 50. Wickramasinghe, L. C. et al. Lung and eye disease develop concurrently in supplemental
664 oxygen-exposed neonatal mice. *American Journal of Pathology*. S0002-9440(20)30287-X (2020).
665

Figure 1

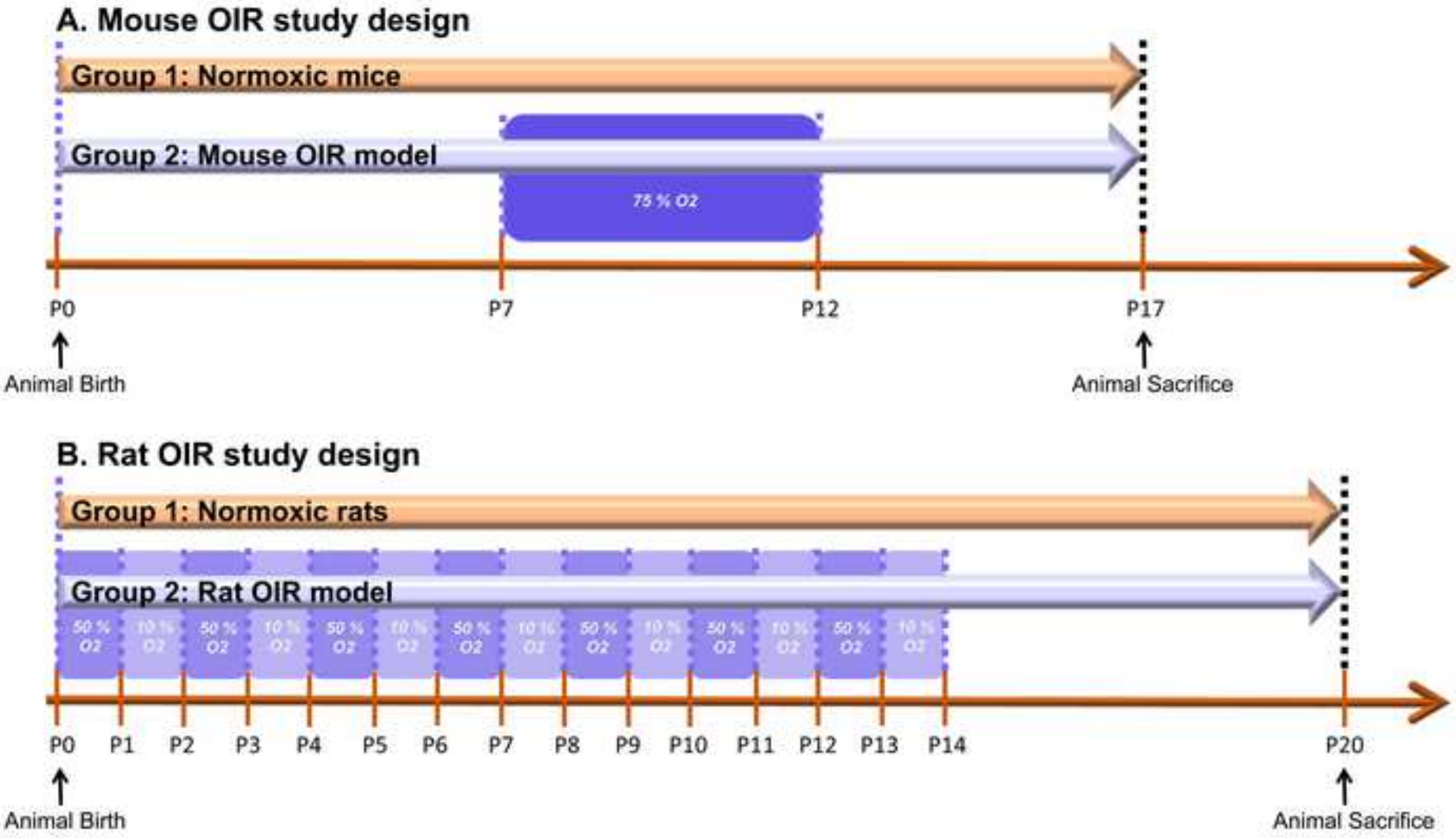

Figure 2

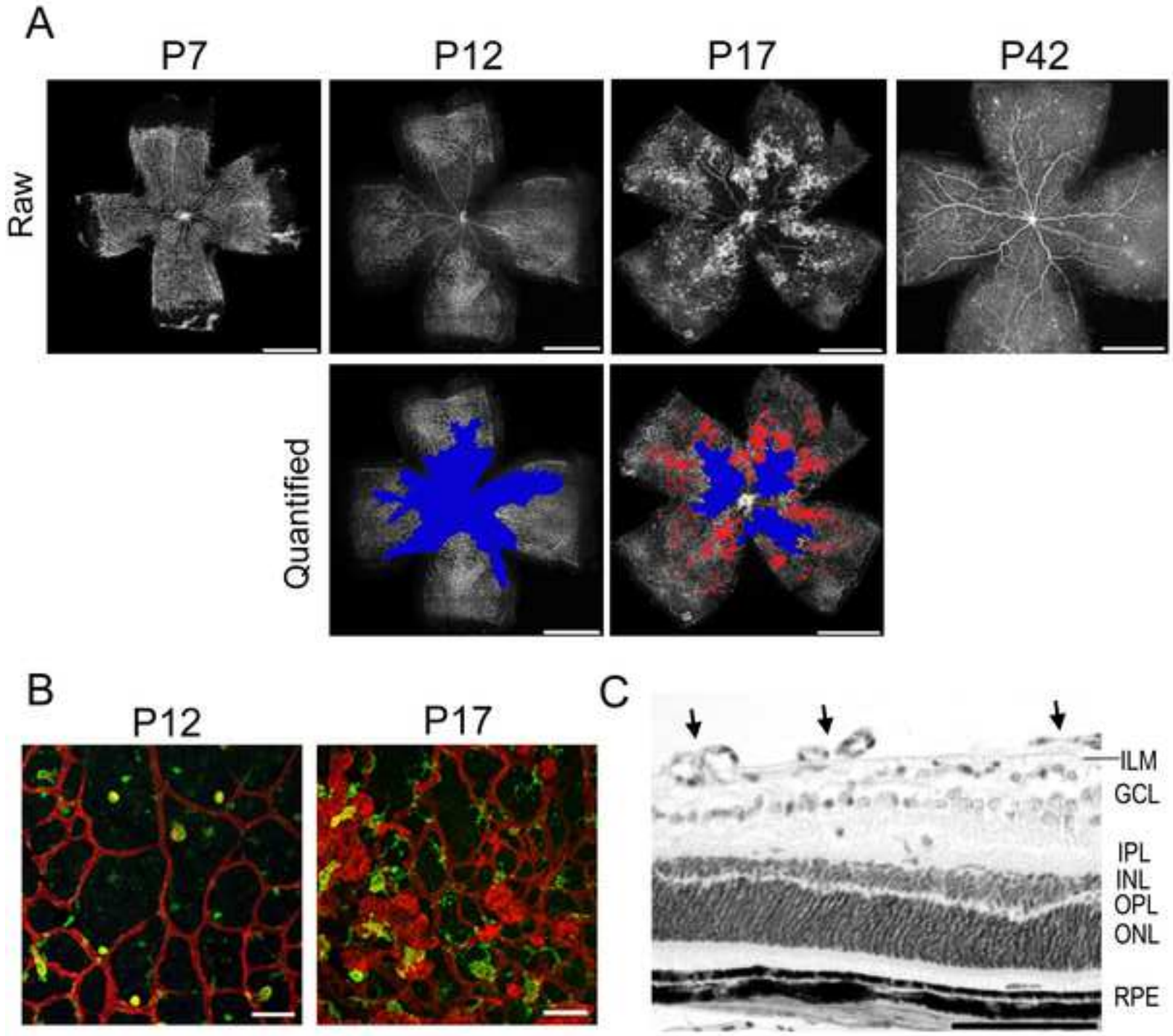

Figure 3

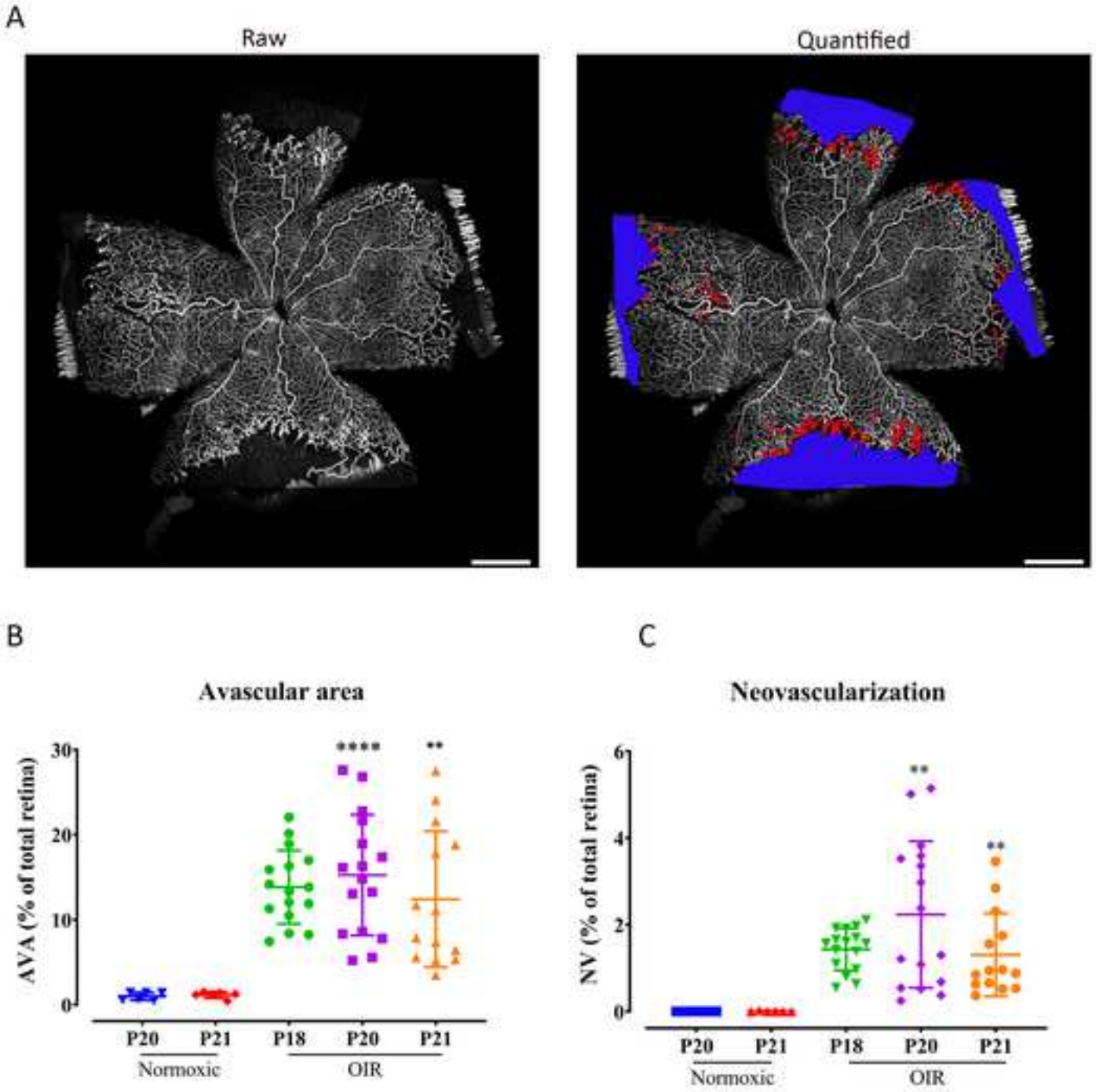

Figure 4

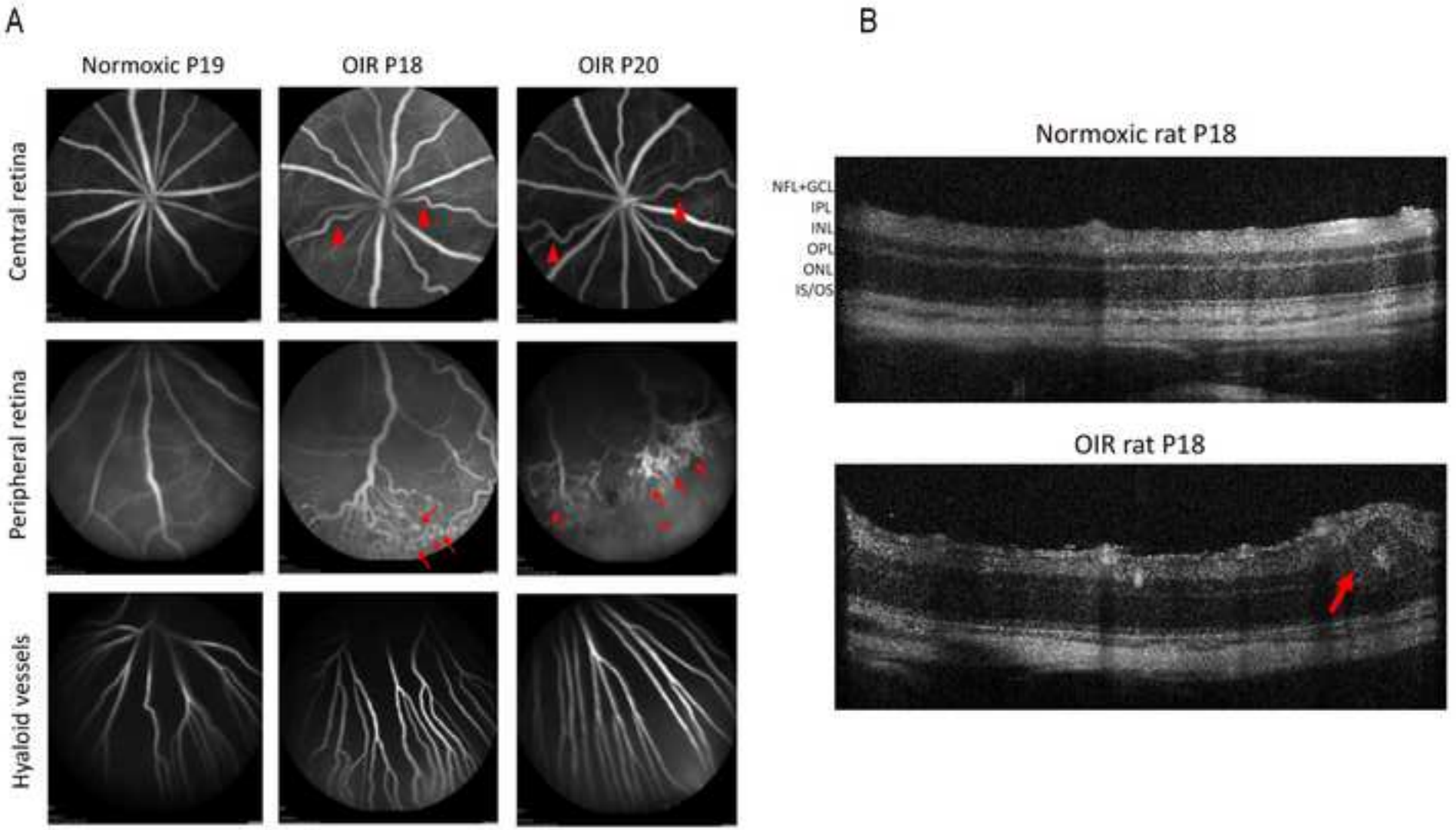

Figure 5

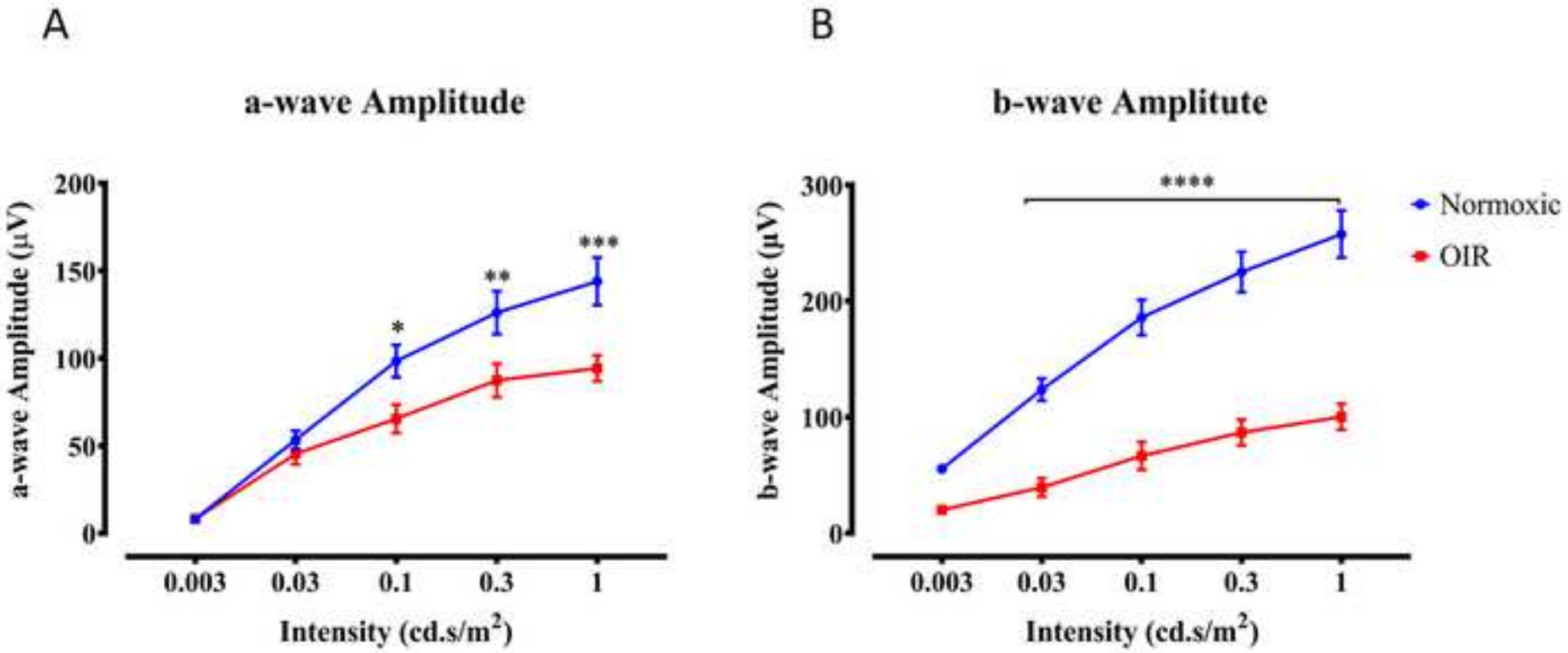

Figure 6

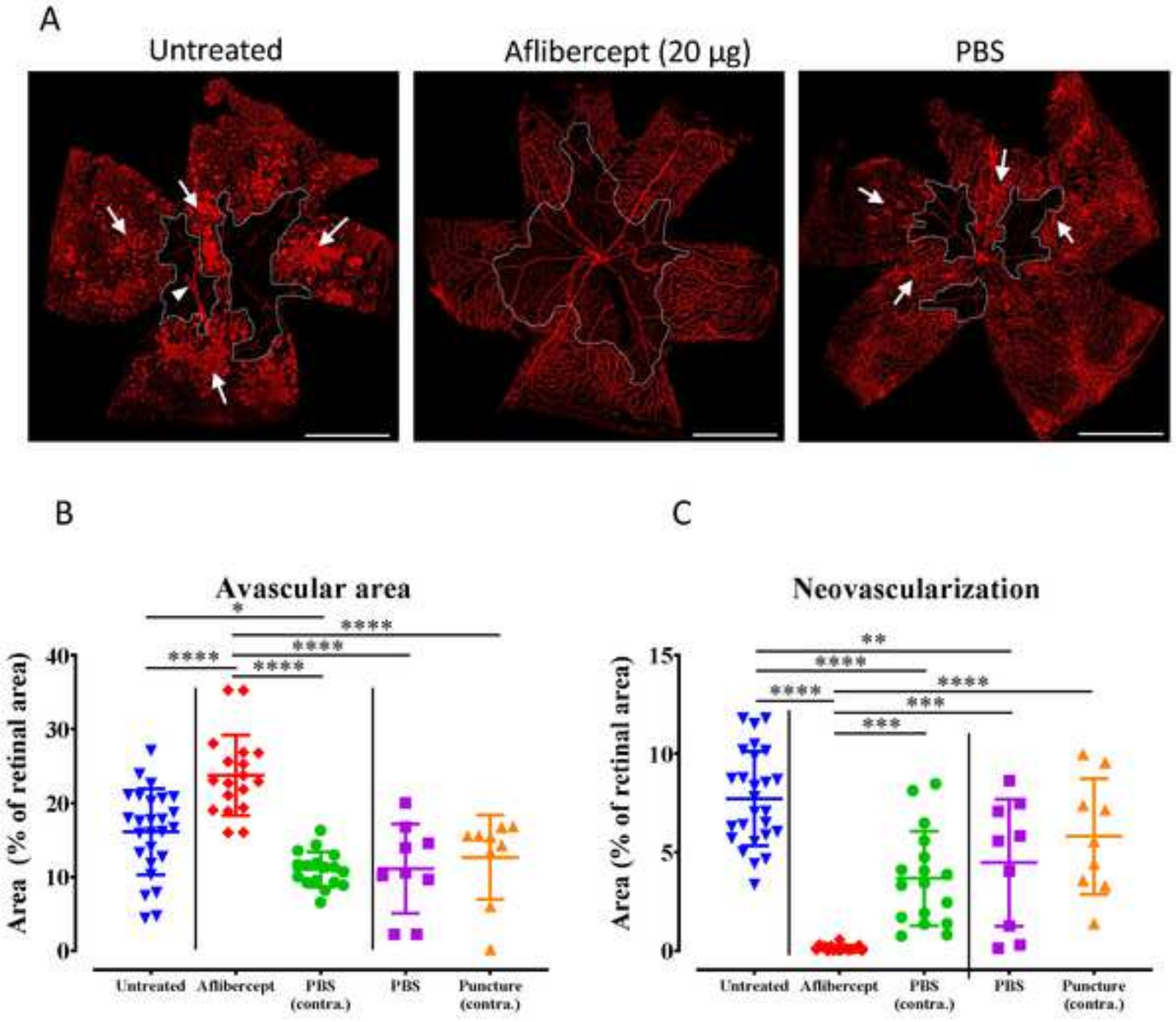

Name of Material/Equipment

33 gauge, Small Hub RN Needle
Adobe Photoshop
Air pump air100
Anaesthesia unit 410 AP
AnalaR NORMAPUR Soda lime
Attane Vet 1000 mg/g
Brush
Carbon dioxide gas
Celeris D430 ERG system
Cell culture dishes
Cepetor Vet 1 mg/mL
Cover slips
O2 Controlled InVivo Cabinet, Aninal Filtrarion System and Dehumidifier
E702 O2 sensor
Envisu R2200 Spectral Domain Optical Coherence Tomograph (SD-OCT)
Eye spears
Flexilux 600LL Cold light source
Fluorescein sodium salt
Gas Exhaust unit (+Double 3-way valve, mouse and rat face masks, UNOsorb filter)
Glass syringe, Model 65 RN
HRA2 Retina angiograph (FA)
Isolectin GS-IB4, Alexa Fluor 488 Conjugate
Ketaminol Vet 50 mg/mL
Medicinal Oxygen gas
Mice C57BL/6JRj
Microscope slides
Minims Povidone Iodine 5% (unit)
Nitrogen gas
Oftan Chlora 10 mg/g
Oftan Metaoksedrin 100 mg/ml
Oftan Obucain 4 mg/ml
Oftan Tropicamid 5 mg/ml
ProOx Model 110 O2 controller and animal chamber

ProOx Model P360 O2 controller and animal chamber
Rats CD(SD)
Revertor 5 mg/mL
Silica gel
Systane Ultra 10ml
Systane Ultra unit 0.7ml
Transfer pipette
VENTI-Line VL 180 PRIME Drying oven
VisiScope SZT350 Stereomicroscope

Company	Catalog Number/Serial Number
Hamilton Company	7803-05, 10mm, 25°, PS4
Adobe Inc.	
Eheim GmbH & Co. KG.	143207
Univentor Ltd.	2360309
VWR International Ltd	22666.362
VET MEDIC ANIMAL HEALTH OY	vnr 17 05 79
Diagnosys LLC	121
Greiner Bio-One International GmbH	664 160
VET MEDIC ANIMAL HEALTH OY	vnr 08 78 96
Thermo Fisher Scientific	15165452
Coy Laboratory Products	
BioSphenix, Ltd.	E207, 1801901
Bioptigen, Inc.	BPN000668
Beaver-Visitec International, Inc.	0008685
Mikron	11140
Merck KGaA	F6377-100G
UNO Roestvaststaal BV	GEX 17015249
Hamilton Company	7633-01
Heidelberg Engineering GmbH	Spec-KT-05488
Thermo Fisher Scientific	I21411
Intervet International B.V.	vnr 51 14 85
Janvier Labs	
Thermo Fisher Scientific	J1800AMNZ
Bausch & Lomb U.K Limited	vnr 24 11 304
Santen Pharmaceutical Co., Ltd.	vnr 55 01 11
Santen Pharmaceutical Co., Ltd.	vnr 55 03 43
Santen Pharmaceutical Co., Ltd.	vnr 55 03 50
Santen Pharmaceutical Co., Ltd.	vnr 04 12 36
BioSphenix, Ltd.	803

BioSphenix, Ltd.	538
Charles River Laboratories	
VET MEDIC ANIMAL HEALTH OY	vnr 13 04 97
Alcon	Tamro 2050250
Alcon	Tamro 2064871
Thermo Fisher Scientific	1343-9108
VWR	VL180S 170301
VWR	481067

Comments/Description

For intravitreal injection
For image analysis
For inhalation anaesthesia
For inhalation anaesthesia
For CO2 control during model induction
For inhalation anaesthesia
For preparation of flat mounts
For sacrifice
For *in vivo ERG*
For preparation of flat mounts
For anaesthesia
For preparation of flat mounts
Closed system for disease model induction, optional for semi-closed system
For oxygen level measurement
For *in vivo* imaging
For intravitreal injection and *in vivo* imaging
For intravitreal injection or tissue collection
For *in vivo* imaging
For inhalation anaesthesia
For intravitreal injection
For *in vivo* imaging
For labeling retinal vasculature on flat mounts
For anaesthesia
For disease model induction
Also other strains possible
For preparation of flat mounts
For intravitreal injection
For disease model induction (rat)
For intravitreal injection
For *in vivo* ERG
For intravitreal injection
For *in vivo* imaging
For disease model induction, semi-closed system, optional for closed system

For disease model induction, semi-closed system, optional for closed system
Also other strains possible
For anaesthesia reversal
For humidity control during model induction
For hydration of the eye
For hydration of the eye
For preparation of flat mounts
For drying silica gel
For intravitreal injection or tissue collection

TAMPEREEN YLIOPISTO
LÄÄKETIETEEN LAITOS

UNIVERSITY OF TAMPERE
MEDICAL SCHOOL

July 15, 2020

Vineeta Bajaj, Ph.D.

Review Editor

JoVE

Dear Review Editor Bajaj,

We hereby submit our re-revised manuscript entitled “Oxygen-induced retinopathy model for ischemic retinal diseases in rodents” to be re-considered for publication in the *JoVE.*

We now feel that we have adequately addressed all editorial queries and the manuscript has improved in the process. Please find our response to the editorial comments attached to this letter below. All authors have read and approved the revised version of the manuscript, its content, and its re-submission to the *JoVE*.

I as a corresponding author, on behalf of all the authors, hereby re-affirm that our manuscript presents original description of research methodology and that it has not been published and is not being considered for publication elsewhere. The authors have provided the full disclosure of their conflict-of-interest. We hope that you find our revised manuscript acceptable for publication in the *JoVE*.

Hannele Uusitalo-Järvinen, M.D., Ph.D.

Chief physician

Tampere Eye Centre

Tampere University Hospital, Tampere, Finland

Phone: +358-44-285 4630 (Cell)

Email: hannele.uusitalo-jarvinen@pshp.fi

Editorial comments:

1. The editor has formatted the manuscript to match the journal's style. Please retain and use the attached version for revision.
.

Reply: *We have retained the journal style in our revisions.*

2. Please address all the specific comments marked in the manuscript.

Reply: *Each query has been addressed. All changes are identified as tracked changes and we have provided a detailed reply to each query in the actual manuscript document.*

3. Once done please ensure that the highlighted section is no more than 2.75 pages including headings and spacings.

Reply: *The highlighted section is well below the page limit.*

4. Please use the dropbox link https://www.dropbox.com/request/eF96pvuf88f1fDrBaQ7N?oref=e to upload all the video files. Please label the files with step numbers.

Reply: *Dr. Vähätupa has uploaded the videos through dropbox link provided above.*

5. Production has reviewed the video files but we will need to see all the files to approve. Presently the only concern is with the screen footage which is not terrible, but ideally, this sort of thing is better suited with a screen capture or locked down-camera with minimal movement and as straight-on as possible.

Reply: *We have provided the missing videos, please see above. We will re-shoot the videos according to instructions provided above if their quality is not acceptable. Please review the videos Dr. Vähätupa has uploaded.*

6. Please select the filming location as Tampere only.

Reply: *The filming location has been changes as suggested above.*

jove JOURNAL OF VISUALIZED EXPERIMENTS
1 Alewife Center #200
Cambridge, MA 02140
tel. 617.945.9051
www.jove.com

ARTICLE AND VIDEO LICENSE AGREEMENT

Title of Article:	Oxygen-induced retinopathy (OIR) in rodents: a pathological neovascularization model for ischemic retinal diseases
Author(s):	Maria Vähätupa[1,2], Niina Jääskeläinen[2], Marc Cerrada-Gimenez[2], Rubina Thapa[2], Tero A.H Järvinen[1], Giedrius Kalesnykas[2], and Hannele Uusitalo-Järvinen

Item 1: The Author elects to have the Materials be made available (as described at http://www.jove.com/publish) via:

☒ ☐ Standard Access ☐ Open Access

Item 2: Please select one of the following items:

☐ ☒ The Author is **NOT** a United States government employee.

☐ The Author is a United States government employee and the Materials were prepared in the course of his or her duties as a United States government employee.

ARTICLE AND VIDEO LICENSE AGREEMENT

1. **Defined Terms.** As used in this Article and Video License Agreement, the following terms shall have the following meanings: "**Agreement**" means this Article and Video License Agreement; "**Article**" means the article specified on the last page of this Agreement, including any associated materials such as texts, figures, tables, artwork, abstracts, or summaries contained therein; "**Author**" means the author who is a signatory to this Agreement; "**Collective Work**" means a work, such as a periodical issue, anthology or encyclopedia, in which the Materials in their entirety in unmodified form, along with a number of other contributions, constituting separate and independent works in themselves, are assembled into a collective whole; "**CRC License**" means the Creative Commons Attribution-Non Commercial-No Derivs 3.0 Unported Agreement, the terms and conditions of which can be found at: http://creativecommons.org/licenses/by-nc-nd/3.0/legalcode; "**Derivative Work**" means a work based upon the Materials or upon the Materials and other pre-existing works, such as a translation, musical arrangement, dramatization, fictionalization, motion picture version, sound recording, art reproduction, abridgment, condensation, or any other form in which the Materials may be recast, transformed, or adapted; "**Institution**" means the institution, listed on the last page of this Agreement, by which the Author was employed at the time of the creation of the Materials; "**JoVE**" means MyJove Corporation, a Massachusetts corporation and the publisher of The Journal of Visualized Experiments; "**Materials**" means the Article and / or the Video; "**Parties**" means the Author and JoVE; "**Video**" means any video(s) made by the Author, alone or in conjunction with any other parties, or by JoVE or its affiliates or agents, individually or in collaboration with the Author or any other parties, incorporating all or any portion of the Article, and in which the Author may or may not appear.

2. **Background.** The Author, who is the author of the Article, in order to ensure the dissemination and protection of the Article, desires to have the JoVE publish the Article and create and transmit videos based on the Article. In furtherance of such goals, the Parties desire to memorialize in this Agreement the respective rights of each Party in and to the Article and the Video.

3. **Grant of Rights in Article.** In consideration of JoVE agreeing to publish the Article, the Author hereby grants to JoVE, subject to **Sections 4** and **7** below, the exclusive, royalty-free, perpetual (for the full term of copyright in the Article, including any extensions thereto) license (a) to publish, reproduce, distribute, display and store the Article in all forms, formats and media whether now known or hereafter developed (including without limitation in print, digital and electronic form) throughout the world, (b) to translate the Article into other languages, create adaptations, summaries or extracts of the Article or other Derivative Works (including, without limitation, the Video) or Collective Works based on all or any portion of the Article and exercise all of the rights set forth in (a) above in such translations, adaptations, summaries, extracts, Derivative Works or Collective Works and(c) to license others to do any or all of the above. The foregoing rights may be exercised in all media and formats, whether now known or hereafter devised, and include the right to make such modifications as are technically necessary to exercise the rights in other media and formats. If the "Open Access" box has been checked in **Item 1** above, JoVE and the Author hereby grant to the public all such rights in the Article as provided in, but subject to all limitations and requirements set forth in, the CRC License.

4. **Retention of Rights in Article.** Notwithstanding the exclusive license granted to JoVE in **Section 3** above, the Author shall, with respect to the Article, retain the non-exclusive right to use all or part of the Article for the non-commercial purpose of giving lectures, presentations or teaching classes, and to post a copy of the Article on the Institution's website or the Author's personal website, in each case provided that a link to the Article on the JoVE website is provided and notice of JoVE's copyright in the Article is included. All non-copyright intellectual property rights in and to the Article, such as patent rights, shall remain with the Author.

5. **Grant of Rights in Video – Standard Access.** This **Section 5** applies if the "Standard Access" box has been checked in **Item 1** above or if no box has been checked in **Item 1** above. In consideration of JoVE agreeing to produce, display or otherwise assist with the Video, the Author hereby acknowledges and agrees that, Subject to **Section 7** below, JoVE is and shall be the sole and exclusive owner of all rights of any nature, including, without limitation, all copyrights, in and to the Video. To the extent that, by law, the Author is deemed, now or at any time in the future, to have any rights of any nature in or to the Video, the Author hereby disclaims all such rights and transfers all such rights to JoVE.

6. **Grant of Rights in Video – Open Access.** This **Section 6** applies only if the "Open Access" box has been checked in **Item 1** above. In consideration of JoVE agreeing to produce, display or otherwise assist with the Video, the Author hereby grants to JoVE, subject to **Section 7** below, the exclusive, royalty-free, perpetual (for the full term of copyright in the Article, including any extensions thereto) license (a) to publish, reproduce, distribute, display and store the Video in all forms, formats and media whether now known or hereafter developed (including without limitation in print, digital and electronic form) throughout the world, (b) to translate the Video into other languages, create adaptations, summaries or extracts of the Video or other Derivative Works or Collective Works based on all or any portion of the Video and exercise all of the rights set forth in (a) above in such translations, adaptations, summaries, extracts, Derivative Works or Collective Works and (c) to license others to do any or all of the above. The foregoing rights may be exercised in all media and formats, whether now known or hereafter devised, and include the right to make such modifications as are technically necessary to exercise the rights in other media and formats. For any Video to which this **Section 6** is applicable, JoVE and the Author hereby grant to the public all such rights in the Video as provided in, but subject to all limitations and requirements set forth in, the CRC License.

7. **Government Employees.** If the Author is a United States government employee and the Article was prepared in the course of his or her duties as a United States government employee, as indicated in **Item 2** above, and any of the licenses or grants granted by the Author hereunder exceed the scope of the 17 U.S.C. 403, then the rights granted hereunder shall be limited to the maximum rights permitted under such statute. In such case, all provisions contained herein that are not in conflict with such statute shall remain in full force and effect, and all provisions contained herein that do so conflict shall be deemed to be amended so as to provide to JoVE the maximum rights permissible within such statute.

8. **Protection of the Work.** The Author(s) authorize JoVE to take steps in the Author(s) name and on their behalf if JoVE believes some third party could be infringing or might infringe the copyright of either the Author's Article and/or Video.

9. **Likeness, Privacy, Personality.** The Author hereby grants JoVE the right to use the Author's name, voice, likeness, picture, photograph, image, biography and performance in any way, commercial or otherwise, in connection with the Materials and the sale, promotion and distribution thereof. The Author hereby waives any and all rights he or she may have, relating to his or her appearance in the Video or otherwise relating to the Materials, under all applicable privacy, likeness, personality or similar laws.

10. **Author Warranties.** The Author represents and warrants that the Article is original, that it has not been published, that the copyright interest is owned by the Author (or, if more than one author is listed at the beginning of this Agreement, by such authors collectively) and has not been assigned, licensed, or otherwise transferred to any other party. The Author represents and warrants that the author(s) listed at the top of this Agreement are the only authors of the Materials. If more than one author is listed at the top of this Agreement and if any such author has not entered into a separate Article and Video License Agreement with JoVE relating to the Materials, the Author represents and warrants that the Author has been authorized by each of the other such authors to execute this Agreement on his or her behalf and to bind him or her with respect to the terms of this Agreement as if each of them had been a party hereto as an Author. The Author warrants that the use, reproduction, distribution, public or private performance or display, and/or modification of all or any portion of the Materials does not and will not violate, infringe and/or misappropriate the patent, trademark, intellectual property or other rights of any third party. The Author represents and warrants that it has and will continue to comply with all government, institutional and other regulations, including, without limitation all institutional, laboratory, hospital, ethical, human and animal treatment, privacy, and all other rules, regulations, laws, procedures or guidelines, applicable to the Materials, and that all research involving human and animal subjects has been approved by the Author's relevant institutional review board.

11. **JoVE Discretion.** If the Author requests the assistance of JoVE in producing the Video in the Author's facility, the Author shall ensure that the presence of JoVE employees, agents or independent contractors is in accordance with the relevant regulations of the Author's institution. If more than one author is listed at the beginning of this Agreement, JoVE may, in its sole

discretion, elect not take any action with respect to the Article until such time as it has received complete, executed Article and Video License Agreements from each such author. JoVE reserves the right, in its absolute and sole discretion and without giving any reason therefore, to accept or decline any work submitted to JoVE. JoVE and its employees, agents and independent contractors shall have full, unfettered access to the facilities of the Author or of the Author's institution as necessary to make the Video, whether actually published or not. JoVE has sole discretion as to the method of making and publishing the Materials, including, without limitation, to all decisions regarding editing, lighting, filming, timing of publication, if any, length, quality, content and the like.

12. **Indemnification.** The Author agrees to indemnify JoVE and/or its successors and assigns from and against any and all claims, costs, and expenses, including attorney's fees, arising out of any breach of any warranty or other representations contained herein. The Author further agrees to indemnify and hold harmless JoVE from and against any and all claims, costs, and expenses, including attorney's fees, resulting from the breach by the Author of any representation or warranty contained herein or from allegations or instances of violation of intellectual property rights, damage to the Author's or the Author's institution's facilities, fraud, libel, defamation, research, equipment, experiments, property damage, personal injury, violations of institutional, laboratory, hospital, ethical, human and animal treatment, privacy or other rules, regulations, laws, procedures or guidelines, liabilities and other losses or damages related in any way to the submission of work to JoVE, making of videos by JoVE, or publication in JoVE or elsewhere by JoVE. The Author shall be responsible for, and shall hold JoVE harmless from, damages caused by lack of sterilization, lack of cleanliness or by contamination due to the making of a video by JoVE its employees, agents or independent contractors. All sterilization, cleanliness or decontamination procedures shall be solely the responsibility of the Author and shall be undertaken at the Author's expense. All indemnifications provided herein shall include JoVE's attorney's fees and costs related to said losses or damages. Such indemnification and holding harmless shall include such losses or damages incurred by, or in connection with, acts or omissions of JoVE, its employees, agents or independent contractors.

13. **Fees.** To cover the cost incurred for publication, JoVE must receive payment before production and publication of the Materials. Payment is due in 21 days of invoice. Should the Materials not be published due to an editorial or production decision, these funds will be returned to the Author. Withdrawal by the Author of any submitted Materials after final peer review approval will result in a US$1,200 fee to cover pre-production expenses incurred by JoVE. If payment is not received by the completion of filming, production and publication of the Materials will be suspended until payment is received.

14. **Transfer, Governing Law.** This Agreement may be assigned by JoVE and shall inure to the benefits of any of JoVE's successors and assignees. This Agreement shall be governed and construed by the internal laws of the Commonwealth of Massachusetts without giving effect to any conflict of law provision thereunder. This Agreement may be executed in counterparts, each of which shall be deemed an original, but all of which together shall be deemed to me one and the same agreement. A signed copy of this Agreement delivered by facsimile, e-mail or other means of electronic transmission shall be deemed to have the same legal effect as delivery of an original signed copy of this Agreement.